Kent Academic Repository

Relativistic Quantum Revivals

P. Strange

School of Physical Sciences, University of Kent, Canterbury, Kent, CT2 7NH, United Kingdom
(Received 23 November 2009; published 26 March 2010)

Quantum revivals are now a well-known phenomena within nonrelativistic quantum theory. In this Letter we display the effects of relativity on revivals and quantum carpets. It is generally believed that revivals do not occur within a relativistic regime. Here we show that while this is generally true, it is possible, in principle, to set up wave packets with specific mathematical properties that do exhibit exact revivals within a fully relativistic theory.

I. Introduction.—A fundamental feature of the physics of waves is interference. It is manifest in all areas of physics. The formation of highly regular spatiotemporal patterns in the quantum mechanical probability density of confined particles is a striking example. The density distributions have been termed "quantum carpets" and have been studied extensively in a number of scalar potential models [1–4]. A much studied model is the particle in a box. Berry [5–8] has used this system to demonstrate full and fractional quantum revivals (the Talbot effect), quantum carpets, and to exhibit fractal behavior of a Schrödinger wave function [9,10]. A number of mathematical descriptions of the patterning of quantum carpets have been developed. It can be described in terms of Wigner functions [2], Green's functions [11], or probability averaging [12]. The mathematical complexity in these cases can obscure the essentially simple pattern formation mechanism which is pairwise interference between particular eigenstates of the system. An excellent review has been provided by Robinett [13]. Practical applications of the Talbot effect are in light [14] and Bose-Einstein condensates [15]. Surprisingly, most systems describing quantum carpets to date have been based on the Schrödinger equation and its solutions. There has been no generalization to the relativistic Dirac equation, although a good approximate treatment of relativistic effects has been examined [16]. It is generally believed that relativity destroys the coherence that leads to the Talbot effect. Here we demonstrate that this is not necessarily true by setting up a simple model for which the Dirac equation has exact analytic solutions and investigating their coherence. We examine the nonrelativistic limit and observe the expected quantum carpet behavior. We then show how this is modified when relativity plays a significant role.

II. Theory.—The Dirac equation in the standard representation [17] describing a particle of mass M is

$$i\hbar \frac{\partial}{\partial t} \Psi(\mathbf{r}, t) = c\boldsymbol{\alpha}.\hat{\mathbf{p}}\Psi(\mathbf{r}, t) + \beta Mc^2\Psi(\mathbf{r}, t). \quad (1)$$

Here α and β are the usual relativistic matrices in the standard representation [17] and all other symbols have

their usual meaning. Difficulties with the boundary conditions for the four component wave function of relativistic quantum theory mean that a "particle in a box" is not an appropriate system in which to discuss revivals. Instead we have chosen a one-dimensional Dirac equation in which the particle is confined to move in a circle of radius R. Then the Dirac equation in circular coordinates has ϕ as the only space variable which varies between 0 and 2π. This is nonphysical, but it is exactly soluble and enables us to examine relativistic effects in quantum carpets in a simple system. The positive energy solution for one spin direction is

$$\Psi(\phi, t) = \sqrt{\frac{3}{2\pi}} \frac{A}{\pi} \sum_{m=\pm\text{occ}} \left(\frac{\hbar\omega_m + Mc^2}{2\hbar\omega_m}\right)^{1/2} \frac{(-1)^m}{m}$$
$$\times \begin{pmatrix} e^{im\phi} \\ 0 \\ 0 \\ \frac{ic\hbar m/R}{\hbar\omega_m + Mc^2} e^{im\phi} \end{pmatrix} e^{-i\omega_m t}, \quad (2)$$

with

$$\omega_m = c\sqrt{\frac{m^2}{R^2} + k_C^2}. \quad (3)$$

Here $k_C = Mc/\hbar$ is the Compton wave vector. The positive square root is taken to determine the frequency. The sum over $m = \pm\text{occ}$ is over all occupied eigenstates and the quantum number m is a nonzero integer. The normalization constant is found numerically from

$$\frac{1}{A^2} = \frac{1}{\pi^2} \sum_{m=\pm\text{occ}} \frac{(-1)^{2m}}{m^2}. \quad (4)$$

This is the wave function we use in what follows. The opposite spin and negative energy states behave similarly.

III. Results.—We examine the evolution of the wave function on a circular orbit in a number of limits. Throughout the results were generated in relativistic units $m = c = h = 1$ unless otherwise stated.

A. Nonrelativistic limit. To take the nonrelativistic limit of these equations we let $c \to \infty$ and require that the values of m that contribute to the summations are such that $|\hbar mc/R| \ll Mc^2$. The summation is over the lowest m_{max} values of m. In this limit the square root quantity in Eq. (2) becomes unity and the frequency becomes

$$\omega_m = c\sqrt{\frac{m^2}{R^2} + k_C^2} \to \frac{2\pi Mc^2}{h} + \frac{\pi m^2}{T}\left(1 - \frac{m^2 h}{4TMc^2}\right), \quad (5)$$

where we have defined the unit of time

$$T = \frac{ML^2}{h} \quad (6)$$

and L is the length of the orbit. $2T$ is the revival time. The first term here originates from the rest mass energy. It cancels when we evaluate densities. The second term is identical to that obtained from the Schrödinger equation. Finally the third term is the relativistic correction to order $1/c^2$ which will be discussed later.

The density plotted as a continuous function of space and time in the nonrelativistic limit is shown in Fig. 1. This is an example of a quantum carpet. The diagonal lines can be understood in terms of simple interference phenomena as follows. Putting all the constants together in A_m in Eq. (2) the density can be written as

$$\begin{aligned} P(\phi, t) &= \Psi^\dagger(\phi, t)\Psi(\phi, t) \\ &= \sum_{m,n=\pm\mathrm{occ}} A_m^\dagger A_n e^{i(n-m)\phi} e^{i\pi(m^2-n^2)t/T}. \end{aligned} \quad (7)$$

We observe that if $n = m$ there is no wavelike behavior, and if $n = -m$ we have stationary wave solutions. Now we can select, arbitrarily, pairs of n and m to examine how they contribute to the total interference pattern. For example, if
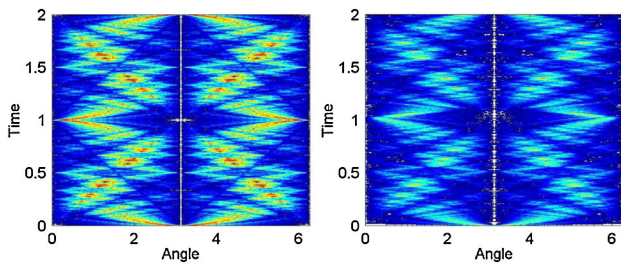

FIG. 1 (color online). Contour maps of the density associated with the wave function of Eq. (2) as a function of time and space. The length of the orbit is chosen as one unit and $m_{max} = 1000$. This is an example of a quantum carpet. Left: The nonrelativistic limit $c = 3 \times 10^5$. For later times the pattern repeats. The nature and fractality of such figures have been discussed in detail [5,9,20,21]. Right: $c = 30$; the pattern does not exactly repeat for later times. Note the diagonal lines that appear and which are described in the text. It can easily be seen that these are well defined in the nonrelativistic limit, but more "washed out" as relativity becomes more important.

we select $m, n = p + 1, -p$, we find

$$\begin{aligned} P_p(\phi, t) &= |A_{p+1}|^2 + |A_{-p}|^2 \\ &\quad + 2A_{p+1}A_{-p}\cos(2p + 1)(\phi - \pi t/T), \end{aligned} \quad (8)$$

which has lines of constant phase when

$$\phi - \frac{\pi t}{T} = \mathrm{const}. \quad (9)$$

It is a key point that this condition is independent of p. In Fig. 2 we show the contribution to the total interference pattern in Fig. 1 from the $m = p + 1$ and $-p$ terms in the summation in Eq. (2) for $p = 2$ and $p = 6$. The gradient of these lines is the same. In particular, note the minimum line from $(\phi, t) = (\pi, 0)$ to $(2\pi, 1)$ occurs for both (and indeed all) values of p and leads to the corresponding diagonal line in Fig. 1. All the diagonal lines in the quantum carpet are due to pairwise interference between terms in the sum of Eq. (7).

B. Ultrarelativistic limit. The limit when the quantum numbers are so large that $\hbar mc/R \gg Mc^2$ can be interpreted simply provided we retain the single-particle interpretation of the Dirac equation. In this limit

$$\omega_m = \frac{mc}{R} + \frac{M^2 Rc^3}{2m\hbar^2} \quad (10)$$

and

$$\Psi(\phi, t) = \sqrt{\frac{3}{4\pi}}\frac{A}{\pi}\sum_{m=\pm\mathrm{occ}}\frac{(-1)^m}{m}\begin{pmatrix}1\\0\\0\\i\end{pmatrix}e^{im(\phi-ct/R)}. \quad (11)$$

The probability density associated with these states is remarkably classical. At $t = 0$ it is localized at $\phi = \pi$. For $t > 0$ it splits into two peaks which travel around the path in opposite directions according to the sign of m. Here all components of the wave function are moving at very close to the speed of light and the wave function does indeed reappear in its original form. In some sense the
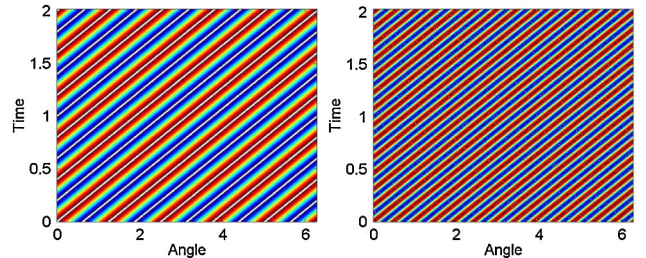

FIG. 2 (color online). The density associated with just two terms in the summation of the wave function of Eq. (2). The terms chosen are $m = p + 1$ and $-p$ for (left) $p = 2$ and (right) $p = 6$. The length of the orbit is chosen as one unit and $c = 3 \times 10^5$. The lines in the interference patterns with $p = 2$ and $p = 6$ are parallel and will undergo coherent interference when included in the full summation in Eq. (2).

Talbot effect survives in this limit. Figure 3 is the ultra-relativistic analogue of Fig. 1 and simply represents particles starting from $\phi = \pi$ and moving at close to the speed of light (and independently of $|m|$) in both directions around the orbit. This can be shown mathematically very easily. At $t = 2T$ the probability density returns to its original form. At $t = T$ there is a mirror image revival, which is identical to the original probability density because of its symmetry at $t = 0$.

C. Relativistic case. Here we examine the case where relativistic effects on coherence cannot be ignored, but are not necessarily dominant. Equation (2) can be simplified by measuring lengths in units of the Compton wavelength and rescaling the time variable $\tau = Mc^2 t/h$ to yield

$$\Psi(\phi, t) = \sum_{m=\pm occ} A_m e^{im\phi} e^{-2\pi i(m^2/q^2+1)^{1/2}\tau}, \qquad (12)$$

where q is the number of Compton wavelengths in the orbit. Every term here has a different value of A_m. Furthermore, the square root in the exponent can be rational or irrational, and so there is no analytic method for performing the summations here. There is no time τ for which the exponent in Eq. (12) is an integer for all values of m. Therefore, quantum revivals do not occur in general. We can examine relativistic corrections to the nonrelativistic limit by including the final term in the binomial expansion in Eq. (5). The general form of the density then becomes

$$P(\phi, t) = \sum_{m,n=\pm occ} A_m^{\dagger} A_n e^{i(n-m)(\phi-(n+m)\pi\{1-[h(n^2+m^2)/4TMc^2]\})t/T} \cdot$$
$$\qquad (13)$$

This is a complicated expression, but insight can be gained from it. To exhibit the effect of relativity we return to the earlier example of pairs of terms $m, n = p + 1, -p$. Now the lines of constant phase are given by

$$\phi - \pi\left(1 - \frac{h}{4TMc^2}(2p^2 + 2p + 1)\right)\frac{t}{T} = \text{const.} \quad (14)$$

Equation (9) is the nonrelativistic limit of Eq. (14). The critical difference between the two equations is that in the relativistic case the lines of constant phase depend on the quantum number p. This shows up in the gradient of the
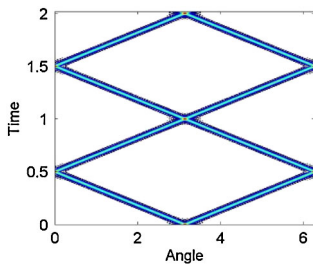

FIG. 3 (color online). The probability density contour map as a function of time and space. This was calculated with $m_{\min} = 950$, $m_{\max} = 1000$, and $c = 1$.

phase lines and is illustrated clearly in Fig. 4. Evidently there will no longer be the coherent interference leading to the diagonal lines that appear in the nonrelativistic quantum carpet of Fig. 1. There are an infinite number of possible relativistic quantum carpets (an example is shown on the left of Fig. 5). In this figure we extend the carpet over two revival times to illustrate the fact that revivals do not, in general, occur within a relativistic framework. An average value of the square of the angular momentum for each pair of states is $J^2 = (n^2 + m^2)\hbar^2/2$. Then the relativistic correction in Eq. (13) is

$$1 - \frac{h(n^2 + m^2)}{4TMc^2} \rightarrow 1 - \frac{J^2}{2M^2R^2} \approx 1 - \frac{v^2}{2c^2}. \qquad (15)$$

We made a binomial expansion in Eq. (13), and on the right-hand side here are the first two terms in the binomial expansion of $(1 - v^2/c^2)^{1/2}$. This line of reasoning yields insight into the breakdown of revivals within relativistic theory. In the nonrelativistic case all components of the wave move along a path that allows them to re-form the original wave function at integer multiples of the revival time. In the relativistic case this is disrupted because the time taken by each component (value of m) of the wave differs from the nonrelativistic case due to time dilation. Hence the constructive interference necessary for the original wave function to be re-formed cannot occur.

D. Exact relativistic revivals. It is possible to construct wave packets that do exhibit full quantum revivals in a fully relativistic theory. Considering Eq. (12), we can set $\theta = \tau/q$ and then

$$\Psi(\phi, t) = \sum_{m=\pm occ} A_m e^{im\phi} e^{-2\pi i(m^2+q^2)^{1/2}\theta}. \qquad (16)$$

Here A_m is a four component column matrix. Now whether or not a revival occurs depends on whether we can construct a wave packet and orbit such that m and q are the lower two elements of Pythagorean triples and such that q, which represents the size of the orbit, is common to all of
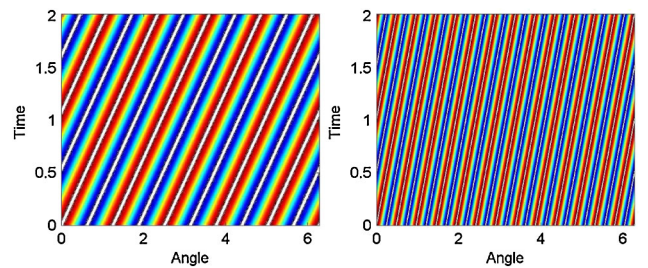

FIG. 4 (color online). The density associated with just two terms in the summation of the wave function (2). The terms chosen are $m = p + 1$ and $-p$ for (left) $p = 2$ and (right) $p = 6$. The length of the orbit is chosen as one unit and $c = 1$. The lines in the interference patterns with $p = 2$ and $p = 6$ are not parallel as they are in the nonrelativistic case and will not undergo the coherent interference when included in the full summation in Eq. (2).
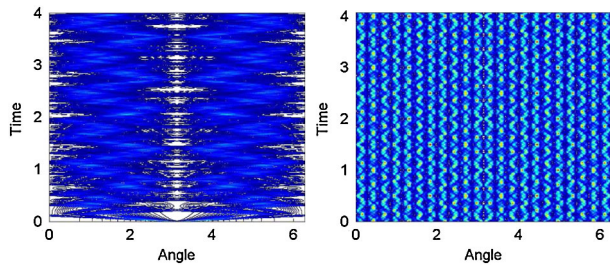
FIG. 5 (color online).   The probability density contour map as a function of time and space with $c = 5$ and 2 revival times. Left: $n_{max} = 1000$. The upper half of the figure does not repeat the lower half. The parameter values were chosen to emphasize that exact revivals do not, in general, occur within a relativistic regime. Right: Calculated for an orbit of length 60 Compton wavelengths. The wave packet was composed only of eigenstates with quantum numbers that form a Pythagorean triple with 60: i.e., $m = \pm 11$, 25, 32, 45, 63, 80, 91, 144, 175, 221, 297, 448, and 899. This probability density repeats exactly each relativistic revival time hq/Mc^2.

the Pythagorean triples in our summation. Formulating the problem in this way removes all dependence of the phase of the wave packet on the speed of light. The speed of light only appears in the units and in the coefficients A_m which govern the amplitude of the wave and so becomes a scale factor that allows us to determine the absolute size of the orbit. Any Pythagorean triple (a, b, c) can be composed from three integers k, m, and n using Euclid's formulas $a = k(n^2 - m^2)$, $b = 2knm$, $c = k(n^2 + m^2)$. By choosing k, n, and m to be all possible permutations of triplets that multiply together to form $q/2$ and for which $n^2 - m^2$ is positive, we generate many (but not necessarily all) acceptable Pythagorean triples. In the right-hand picture in Fig. 5 we present a quantum carpet calculated in this way for $q = 60$. This figure repeats exactly after each relativistic revival time hq/Mc^2.

IV. Conclusions.—In this Letter we have developed a theory of relativistic quantum revivals and shown that exact revivals can occur within a relativistic framework. This can occur in two ways: (i) the physically trivial case where all components of the wave essentially travel at the speed of light and so reproduce themselves exactly after some time and (ii) the case where (in suitably scaled units) the wave packet is formed of eigenstates whose quantum numbers form a Pythagorean triple with the length of the orbit measured in Compton wavelengths. While setting up such a well-defined wave packet would be extremely challenging, one can conceive of observing such behavior in

the charge-carrying quasiparticles in graphene [18] or in a strongly confined pulse of light [19]

[1] O. M. Friesch, I. Marzoli, and W. P. Schleich, New J. Phys. **2**, 4 (2000).
[2] I. Marzoli, F. Saif, I. Bialynicki-Birula, O. M. Friesch, A. E. Kaplan, and W. P. Schleich, Acta Phys. Slovaca **48**, 323 (1998).
[3] D. L. Aronstein and C. R. Stroud, Phys. Rev. A **55**, 4526 (1997).
[4] I. Sh Averbukh and N. F. Perelman, Phys. Lett. A **139**, 449 (1989).
[5] M. V. Berry, J. Phys. A **29**, 6617 (1996).
[6] M. V. Berry, Quantum and Optical Arithmetic and Fractals, http://www.phy.bris.ac.uk/people/berry_mv/the_papers/berry283.pdf.
[7] J. H. Hannay and M. V. Berry, Physica (Amsterdam) **1D**, 267 (1980).
[8] M. V. Berry and S. Klein, J. Mod. Opt. **43**, 2139 (1996).
[9] K. Falconer, *Fractal Geometry* (Wiley, Blackwell. England, 2003).
[10] M. V. Berry and Z. V. Lewis, Proc. R. Soc. A **370**, 459 (1980).
[11] I. Marzoli, I. Bialynicki-Birula, O. M. Friesch, A. E. Kaplan, and W. P. Schleich, in *Proceedings of the PRL Golden Jubilee Conference on Nonlinear Dynamics and Computational Physics*, edited by V. B. Sheorey (Narosa Publishing House, New Delhi, 1999).
[12] J. Marklof, *Limit Theorems for Theta Sums with Applications in Quantum Mechanics* (Shaker-Verlag, Aachen, 1997).
[13] R. W. Robinett, arXiv:quant-ph/0401031v1.
[14] W. B. Case, M. Tomandl, S. Deachapunya, and M. Arndt, Opt. Express **17**, 20 966 (2009).
[15] S. Chio, K. Burnett, O. M. Friesch, B. Kneer, and W. P. Schleich, arXiv:cond-mat/0011468.
[16] I. Marzoli, A. E. Kaplan, F. Saif, and W. P. Schleich, Fortschr. Phys. **56**, 967 (2008).
[17] P. Strange, *Relativistic Quantum Mechanics* (Cambridge University Press, Cambridge, England, 1998).
[18] K. S. Novoselov, A. K. Geim, S. V. Morozov, D. Jiang, I. V. Grigorieva, S. V. Dubonos, and A. A. Firsov, Nature (London) **438**, 197 (2005).
[19] J. Otterbach, P. G. Unanyan, and M. Fleischhauer, Phys. Rev. Lett. **102**, 063602 (2009).
[20] T. M. Apostol, *Introduction to Analytic Number Theory* (Springer-Verlag, New York, 1986).
[21] S. Lang, *Algebraic Number Theory* (Springer, New York, 2000).